

Silver ion concentration dependent properties of silver nanostructured nanocomposite films

S. DEB*, D. SARKAR

Department of Physics, Gauhati University, Guwahati-781014, Assam, India

Structure, morphology, optical and electrical properties of silver nanostructured nanocomposites synthesized for various concentrations of silver salt are studied. The composites have been developed in polyvinyl alcohol matrix. Change in silver ion concentration has been realized by changing AgNO_3 concentration in the reactants. X-ray diffraction patterns show a characteristic peak for silver nanoparticles at $2\theta = 38^\circ$. Infrared spectra reveal the evidence of silver- PVA cross-linking. Scanning electron microscopy shows evidence of near spherical particles with increasing size from 20 to 100 nm with the increase in AgNO_3 concentration. UV-Visible absorption spectra show strong surface plasmon resonance peak in the region of 423-441 nm, a consequence of development of nano-sized Ag particles. Photoluminescence spectra show emission peak at 622-623 nm. Electrical property measured through current-voltage characteristics exhibit ohmic behaviour.

(Received February 15, 2017; accepted April 8, 2019)

Keywords: Silver, Nanoparticles, Plasmon resonance, Photoluminescence, Polymer composite

1. Introduction

It is known that metal nanocomposites can exhibit extraordinary electrical and optical properties which are distinctly different from those of the bulk [1, 2]. Recently, the synthesis of metal nanoparticles through different routes has become an important area of research and development because of rapid developments in the fields of nano-electronics [3, 4] and nano-bioelectronics [5]. Desired electrical and optical properties of the novel metal nanoparticles can be achieved when the process of synthesis has a mechanism for tailoring the size, shape and morphology of the nanoparticles. A large number of reports are available on the synthesis of metal nanoparticles in solution by different methods, such as photochemical [6–8], electrochemical [9–11], chemical reduction [12–18], microwave processing [19], ultra-sound processing [20], gamma irradiation [21–25], ion irradiation [26], plasma processing [27], ball milling process [28] and green synthesis [29–31] etc. Major hindrance in the process of synthesis of such low dimensional particles is the fact that with elapse of time these nanoparticles usually tend to coalesce to develop into larger sized particles due to electrostatic interaction across the Debye double layer. To improve the stability of metal nanoparticles, the most common and convenient, is by dispersing them in a synthetic high polymer matrix [12, 32]. Polyvinyl alcohol (PVA) is one such polymer. It has the advantage over the other such polymers of being water soluble, transparent and has capability of dispersing the nanoparticles in uniform manner. Also, it has the capability to simultaneously act as a reducing agent to form silver nanoparticles from its salt, as well as a stabilizer, so that one obtains homogeneous, transparent film of Ag-PVA nanocomposite. Optical properties of these composite films, viz; UV-Vis absorption spectra depend on particle size [33–36]. So, it becomes of immense importance to

control the size of silver nanoparticles to tailor their optical properties for specific need [37]. In a single composite film also, the particle size may not be uniform. The in-situ size distribution can also be manifested in its photoluminescence behaviour [32]. Among many factors, Ag nano formation largely depends on the concentration of silver ions present, temperature and pH of the reactants [38]. In this article, we aim to visualize the impact on the properties by varying silver ion concentration in the reaction medium. To be particular, we have varied AgNO_3 concentration keeping the concentration of other reagents fixed to search for its effect on shape, size and physical properties of the nanoparticles thus formed.

2. Experimental details

2.1. Materials

Silver nitrate of 99.9% purity is obtained from E. Merk, Germany. PVA (1700-1800 repeat units) is obtained from Sigma chemical Co. and is of very high purity (99.9%). These are used without any further purification. Deionized water has been used as reaction medium although.

2.2. Preparation method

Silver-PVA nanostructured nanocomposites are prepared by chemical reduction of AgNO_3 in presence of PVA. To be particular, AgNO_3 solution is added drop wise to PVA solution (3 wt %) with constant stirring at 90°C . The solution is maintained at that temperature for 1 hr. Completion of the reaction is indicated by the change in colour of the solution to light yellow. Same process is followed for five different concentrations of AgNO_3 (1-5

mM). The resultant solution is spin cast and dried in vacuum to obtain silver-PVA nanocomposite films.

2.3. Structural and optical characterization

XRD data for structure study are collected by Scifert XRD 3000 pd Diffractometer with Cu-K α (0.15418 nm) radiation. FTIR spectra are taken by Perkin Elmer Spectrum RXI-FTIR System. Field emission scanning electron microscope (FESEM) images for morphology and particle size determination are taken by FESEM (JSM-6700F, JEOL, Japan). UV-Vis spectra for optical absorption study are taken by Cary 300 scan UV-Visible spectrophotometer and Photoluminescence (PL) spectra are recorded by F-2500FL spectrometer. Electrical properties of the nanocomposite films are measured through recording current-voltage (I-V) curves by measuring current by Keithly CV meter (model 595) with the supply voltage from its in-built source.

3. Results and discussions

3.1. XRD spectra

XRD pattern of the nanocomposite films are shown in Fig. 1. This shows characteristic peak of silver nano at $2\theta = 38.02^\circ$ for (111) crystalline plane [39].

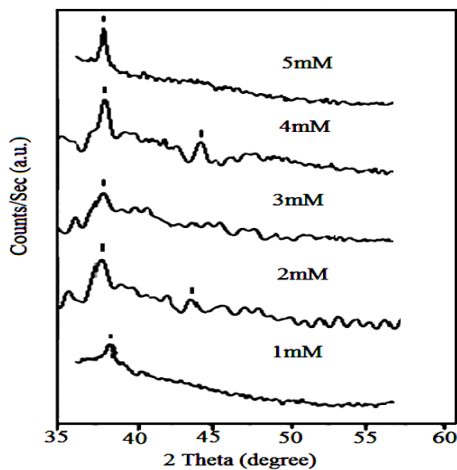


Fig. 1. XRD spectra of Ag-PVA nanocomposites

The broad nature of the XRD peak could be attributed to formation of nanosized particles. From conventional Scherrer formula the average particle size (d) can be written as

$$d = k \lambda / \beta_{1/2} \cos \theta$$

where $\beta_{1/2}$ is full-width at half maximum of the peak at 2θ , k is constant ($k=0.89$) and $\lambda=0.154$ nm is the CuK α_1 wavelength. Considering the (111) plane in the XRD spectrum, value of d is found to be 10-20 nm for AgNO $_3$ concentrations of 1 - 5 mM respectively. Obtained size

from XRD results is much smaller than that obtained from SEM. This may be justified as the particle size calculated by SEM is mostly probing small area of surface, whereas XRD gives a bulk property.

3.2. FTIR spectra

To look for the possible chemical bonding between the PVA and silver nanoparticles, FTIR spectra of these nanocomposite films are recorded. These are shown in Fig. 2, which also shows the spectra for pure PVA for comparison. In the spectrum for pure PVA, the peak for PVA could be assigned by a strong peak at 3460 cm^{-1} for the O-H stretching vibration. This gets shifted in the nanocomposites indicating that silver nanoparticles are bound to the functional group in PVA. Another eminent change in the FTIR spectra of these nanocomposites is the one for the band at 1337 cm^{-1} for PVA. In alcohols, this band is the result of the coupling of the O-H in-plane vibrations at 1420 cm^{-1} with the C-H wagging vibration. Therefore, the decrease in the ratio between the intensities of the band at 1337 cm^{-1} and that at 1420 cm^{-1} with an increase in the content AgNO $_3$ indicates decoupling between the corresponding vibrations due to interaction of the Ag nanoparticles with the O-H groups originating from the PVA chains. The peak at 767 cm^{-1} is due to out-of-plane vibration of O-H group while the band at 837 cm^{-1} corresponds to the out-of-plane vibration of the C-H group. Increase in transmittance of this band with the increase in concentration of AgNO $_3$ indicates interaction between Ag nanoparticles and PVA takes place along O-H group.

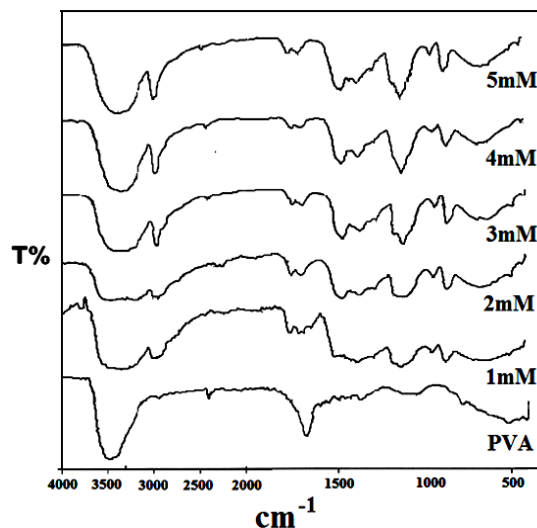


Fig. 2. FTIR spectra of silver-PVA nanocomposites

3.3. SEM images

The film morphology and particle size distribution of Ag-PVA nanocomposite is studied by FESEM images which are shown in Fig. 3. In the inset, the histogram fitted with the Gaussian function of the size distribution of nanoparticles indicates the particle size. Size of the

particles for 1-5 mM are given in Table 1. The pictures show uniform distribution of nanoparticles throughout the film. Further within a particular film, the size of the particles varies but the particles are nearly uniformly spherical in shape. Average particle size is found to

increase from 20 nm to 100 nm with the increase in concentration of AgNO_3 . However, for 1 mM concentration particles are most uniformly distributed and for the 5 mM one, there is a tendency towards making transition from spherical to cubic shape.

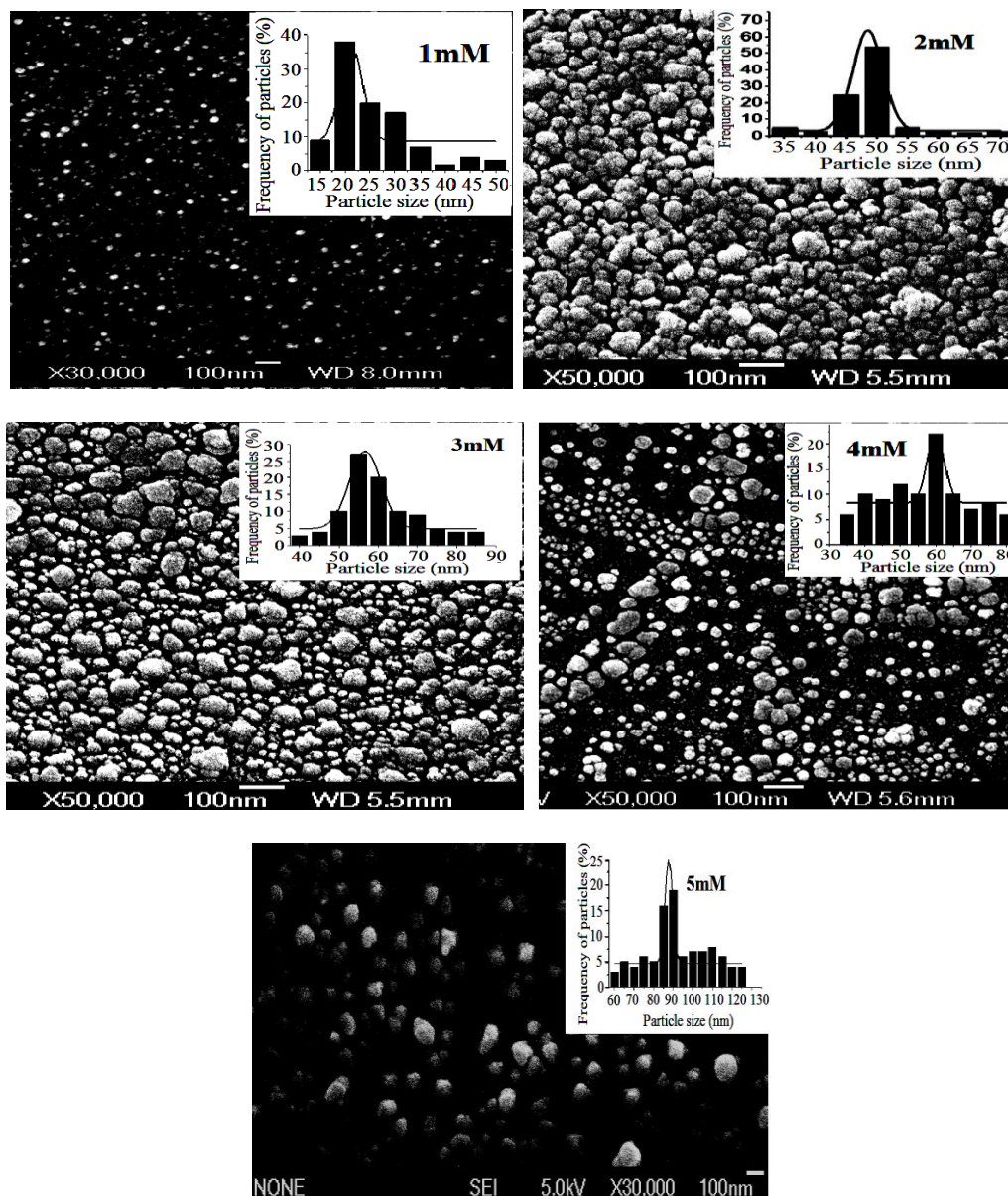


Fig. 3. SEM images of silver-PVA nanocomposites

3.4. UV-visible spectra

In Fig. 4, we show the UV-visible absorption spectra of pure PVA and silver nanoparticles dispersed in PVA for different concentrations. For PVA, the absorption peak is observed at 280 nm. For Silver-PVA nanocomposite, these spectra show strong plasmon resonance peak in the range 423 nm- 441nm which is a clear consequence of formation of nanosized particles [40]. The peaks are seen to blue shift with increase in concentration up to 4 mM and the start shifting towards red. It has been reported that for narrow particle size distribution of silver nano in SiO_2 matrix absorption spectra show homogeneous broadening

whereas for wide particle size distribution the broadening is predicted to be inhomogeneous [41]. In our study, we notice that the absorption curve broadens more towards red region indicating distribution of particle size of little wide range and the absorption peak corresponds to the value for average particle size. We have observed this wide range of particle size for a particular film in the SEM images also.

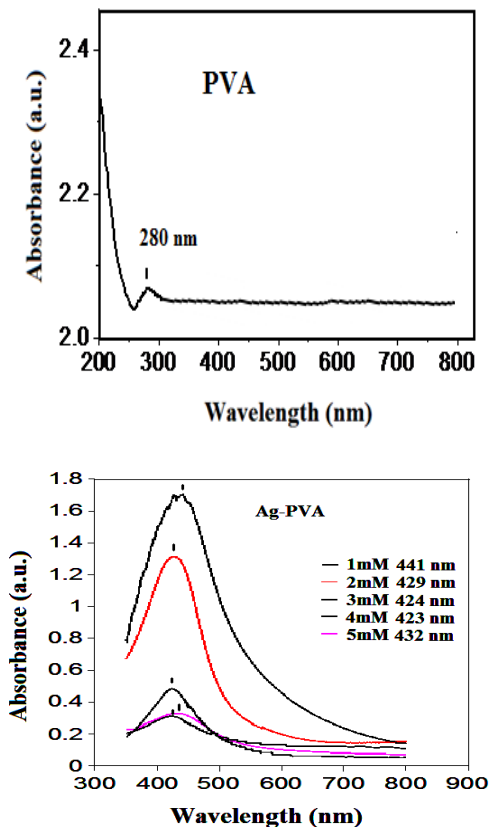


Fig. 4. UV-visible spectra of PVA and Ag-PVA nanocomposites

3.5. Optical band gap in silver-PVA nanocomposite

The maximum absorbance wavelength is associated with the conduction band energy according to quantum theory of metal nanoparticles [42-44]. The band gap can be calculated directly from the UV-visible absorption spectra by using the following Einstein's photon energy equation:

$$E = hc / \lambda_{\max}$$

where λ_{\max} is the maximum absorbance wavelength, h is the Planck constant and c is the speed of light. Calculated band gap for PVA is 4.4 eV and for 1-5mM silver-PVA nanocomposite, band gap is in the range of 2.81-2.93 eV. The Optical band gaps of these Ag-PVA nanocomposite films are obtained from the intercepts of the conventional Tauc plots of $(\alpha(\nu)h\nu)^2$ vs. $h\nu$, $\alpha(\nu)$ being the absorption coefficient. These plots are shown in Fig. 5. Band gap for direct allowed transition may be determined from the extrapolation of the linear section of the curves to x-axis for $(\alpha(\nu)h\nu)^2 = 0$. This will give the band gap of the surface plasmon resonance absorption of electrons in the conduction bands of silver nanoparticles. The band gaps are found to be 4.4 eV for PVA and in the range of 2.35 - 2.56 eV as the AgNO_3 concentration varies from 1 – 5 mM. Similar direct allowed transition is considered for calculating the energy band gap of PVA and silver-polyvinylpyrrolidone (Ag/PVP) nanocomposites [45-47]. The band gap with direct allowed transition results as listed in Table 1 are much closer to that of the direct calculations from Einstein's photon energy Equation.

Table 1. Particle size and optical properties with silver ion concentration

Sl.No.	Silver ion concentration (mM)	Particle size from SEM (nm)	Absorbance maximum wavelength (nm)	Band gap (eV)		
				calculated by Einstein equation (a)	calculated from Tauc plots (b)	Difference (a-b)
1	1	21.5 ± 3.2	441	2.81	2.35	0.46
2	2	48.6 ± 3.1	429	2.89	2.55	0.34
3	3	56.5 ± 5.4	424	2.93	2.56	0.37
4	4	60.0 ± 4.4	423	2.93	2.56	0.37
5	5	87.5 ± 3.1	432	2.87	2.55	0.32

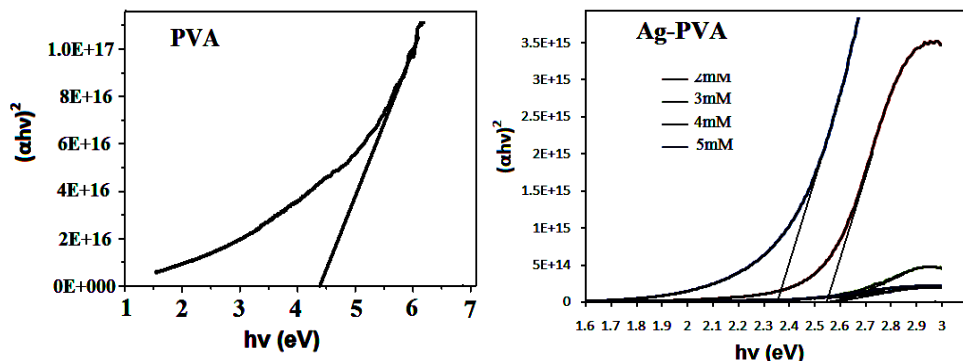


Fig. 5. Band gap of Ag-PVA nanocomposites

3.6. Photoluminescence spectra

The photoluminescence (PL) spectra of silver nano are generally attributed to electronic transition between the highest d- band and sp-conduction band. Room temperature (300K) PL spectra of these Ag-PVA nanocomposite films are shown in Fig 6. The composites containing Ag nanoparticles show emission bands at around 622-623 nm for excitation wavelength of 415 nm. In order to corroborate whether the PL emission is from the embedded Ag nanoparticles or from the matrix (PVA), PL spectra for pure PVA film is also measured. The absence of PL emission band in PVA indicates that PL emission is originating from silver nanoparticles embedded in PVA matrix. This result is similar to what obtained by Zheng et al. [48] for dendrimer-encapsulated silver nanodots.

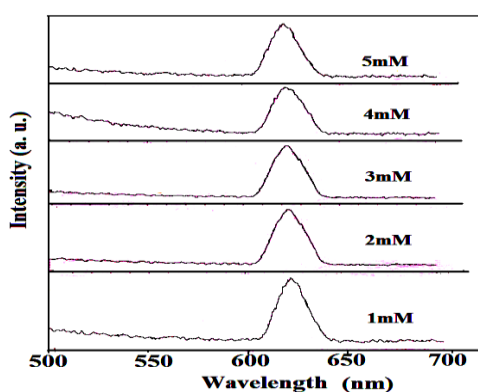


Fig. 6. PL spectra silver-PVA nanocomposites

3.7. I-V characteristics

The electrical properties of Ag-PVA nanocomposite films are measured by I-V curves up to applied voltage of 20 V. These plots are shown in Fig. 7 for in-plane configuration of electrodes. These show ohmic nature with increase in slope with the increase in concentration of silver source. For 5 mM one, the slope of the I-V curve is very large, as the particle size is more than 100 nm which can be due to attainment of near bulk properties. However, similar ohmic behaviour is seen for perpendicular electrode configuration too. For in-plane configuration, on the top of the film two small areas are coated with silver paint and connections are taken by fine copper wires. For perpendicular configuration, the film is spin cast on ITO glass and top electrode is taken as earlier. With the increase in concentration of AgNO₃, the slope of I-V graph is seen to increase indicating increase in conductivity.

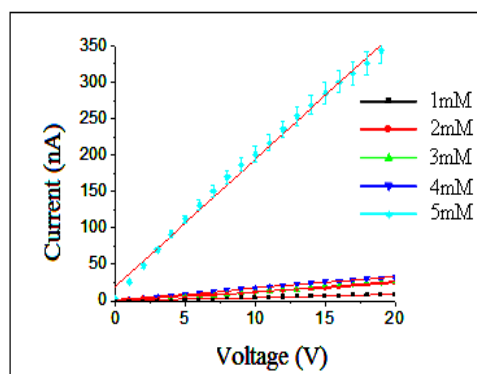


Fig. 7. I-V characteristics silver-PVA nanocomposites

4. Conclusions

Change of concentration of silver source is found to have remarkable effect on the size and physical properties of silver nanostructures. XRD spectra shows the characteristic peak of silver nano at $2\theta = 38.02^\circ$ for (111) crystalline plane. FTIR spectra confirm cross-linking between silver and PVA along -OH functional group. Particle size is seen to increase with increase in concentration. For lowest concentration of AgNO₃ particle distribution is the most uniform and for the highest one, slight change in shape (towards cubic) is observed. UV-Vis absorption spectra show broadening. PL spectra show emission peak at more or less the same position (622-623 nm) for excitation wavelength of 415 nm. I-V curves show ohmic behaviour with increase of slope as the concentration is increased.

References

- [1] G. A. Ozin, *Adv. Mater.* **4**, 612 (1992).
- [2] S. Deb, D. Sarkar, *J. Experimental Nanoscience* **9**, 375 (2014).
- [3] T. Sato, H. Ahmed, D. Brown and B F G Johnson, *J. Appl. Phys.* **82** 696 (1997).
- [4] W. L. Barnes, A. Dereux, T. W. Ebbesen, *Nature* **424**, 824 (2003).
- [5] Y. Cui, Q. Wei, H. Park, C. M. Lieber, *Science* **293**, 1289 (2001).
- [6] H. H. Huang, X. P. Ni, G. L. Loy, C. H. Chew, K. L. Tan, F. C. Loh, J. F. Deng, G. O. Xu, *Langmuir* **12**, 909 (1996).
- [7] F. Mafune, J. Y. Kohno, Y. Takeda, T. Kondow, *J. Phys. Chem. B* **104**, 8333 (2000).
- [8] A. Henglein, *Chem. Mater* **10**, 444 (1998).
- [9] J. J. Zhu, S. W. Lin, O. Palchik, Y. Koltypin, A. Gedanken, *Langmuir* **16**, 6396 (2000).
- [10] Y. Y. Yu, S. S. Chang, C. L. Lee, C. R. Chris Wang, *J. Phys. Chem. B* **101**, 6661 (1997).
- [11] T. R. Manfred, H. Wolfgang, *J. Am. Chem. Soc.* **116**, 7401 (1994).

- [12] S. Deb, D. Sarkar, *Indian J. Phys.* **82**, 715 (2008).
- [13] I. Pastoriza, L. M. Liz-Marzan, *Langmuir* **15**, 948 (1999).
- [14] L. N. Lewis, N. Lewis, *J. Am. Chem. Soc.* **108**, 7228 (1986).
- [15] U. Nickel, A. Z. Castell, K. Poppl, S. Schneider, *Langmuir* **16**, 9087 (2000).
- [16] N. Leopold, B. Lendl, *J. Phys. Chem. B* **107**, 5723 (2003).
- [17] L. Kvitek, R. Prucek, A. Panacek, R. Novtny, J. Hrbac, R. Zboril, *J. Mater. Chem.* **15**, 1099 (2005).
- [18] Y. Saito, J. J. Wang, D. N. Batchelder, D. A. Smith, *Langmuir* **19**, 6857 (2003).
- [19] W. Tu, H. Liu, *Chem. Mater* **12**, 564 (2000).
- [20] Y. Nagata, Y. Watananabe, S. Fujita, T. Dohmaru, S. Taniguchi, *J. Chem. Soc. Chem. Commun.* **21**, 1620 (1992).
- [21] M. K. Temgire, S. S. Joshi, *Radiat. Phys. Chem.* **71**, 1039 (2004).
- [22] W. T. Wu, Y. Wang, L. Shi, Q. Zhu, W. Pang, G. Xu, F. Lu, *Nanotechnology* **16**, 3017 (2005).
- [23] M. Kumar, L. Varshney, *S. Francis, Radiat. Phys. Chem.* **73**, 21 (2005).
- [24] A. Henglein, *Langmuir* **17**, 2329 (2001).
- [25] X. Xu, Y. Yin, X. Ge, H. Wu, Z. Zhang, *Mater. Lett.* **37**, 354 (1998).
- [26] A. L. Stepanov, D. E. Hole, P. D. Townsend, *J. Non-Cryst. Solids* **260**, 65 (1999).
- [27] C. Balasubramanian, V. P. Godbole, V. K. Rohatgi, A. K. Das, S. V. Bhoraskar, *Nanotechnology* **15**, 370 (2004).
- [28] E. Purushotom, N. G. Krishna, *Indian Journal of Physics* **88**(2), 157 (2014).
- [29] D. Saikia, P. K. Gogoi, P. Phukan, N. Bhuyan, S. Borchetia, J. Saikia, *Adv. Mater. Lett.* **6**, 260 (2015).
- [30] B. Kumar, K. Smita, L. Cumbal, A. Debut, J. Camacho, E. H. G. M. de G. López, M. Grijalva, Y. Angulo, G. Rosero, *Adv. Mater. Lett.* **6**, 127 (2015).
- [31] K. M. Ezealisiji, X. S. Noundou, S. E. Ukwueze, *Appl. Nanosci.* **7**, 905 (2017).
- [32] D. Basak, S. Karan, B. Mallik, *Chem. Phys. Lett.* **420**, 115 (2006).
- [33] W. Li, S. Seal, E. Megan, J. Ramsdell, K. Scammon, G. Lelong, L. Lachal, K. A. Richardson, *J. Appl. Phys.* **93**, 9553 (2003).
- [34] A. V. Aiboushev, A. A. Astafiev, Yu. E. Lozovik, S. P. Merkulova, V. A. Nadtochenko, O. M. Sarkisov, M. Willander, *Phys. Status Solidi C* **6**, 162 (2009).
- [35] A. L. González, C. Noguez, *Phys. Status Solidi C* **4**, 4118 (2007).
- [36] S. Deb, D. Sarkar, *Optik* **157**, 1115 (2018).
- [37] Y. Liu, F. Chen, S. M. Kuznicki, R. E. Wasylshen, Z. Xu, *J. Nanosci. Nanotechnol.* **9**, 2768 (2009).
- [38] J. S. Kim, *J. Ind. Eng. Chem.* **13**, 566 (2007).
- [39] A. Swami, P. R. Selvakannan, R. Pasricha, M. Sastri, *J. Phys. Chem. B* **108**, 19269 (2004).
- [40] R. He, X. Qian, J. Yin, Z. K. Zhu, *J. Mater. Chem.* **12**, 3783 (2002).
- [41] K. Kurihara, C. Rockstuhl, T. Nakano, T. Arai, J. Tomonaga, *Nanotechnology* **16**, 1565 (2005).
- [42] E. Saion, E. Gharibshahi, *J. Fundam. Sci.* **7**, 6 (2011).
- [43] N. Soltani, E. Saion, M. Erfani, K. Rezaee, G. Bahmanrokh, G. P. Drummen, A. Bahrami, M. Z. Hussein, *Int. J. Mol. Sci.* **13**, 12412 (2012).
- [44] E. Gharibshahi, E. Saion, *Int. J. Mol. Sci.* **13**, 14723 (2012).
- [45] L. Gharibshahi, E. Saion, E. Gharibshahi, A. H. Shaari, K. A. Matori, *Materials* **10**, 402 (2017).
- [46] S. S. Gasaymeh, S. Radiman, L. Y. Heng, E. Saion, G. H. M. Saeed, *African Physical Review* **4:0006**, 31 (2010).
- [47] S. B. Aziz, *Journal of Electronic Materials* **45**, 1 (2016).
- [48] J. Zheng R. M. Dickson, *J. Am. Chem. Soc.* **124**, 13982 (2002).

*Corresponding author: debsulochana@gauhati.ac.in